Convective Downmixing of Plumes in a Coastal Environment

GREGORY J. MCRAE, FREDRICK H. SHAIR[1] and JOHN H. SEINFELD[1]

Environmental Quality Laboratory, California Institute of Technology, Pasadena 91125

(Manuscript received 30 April 1981, in final form 2 August 1981)

ABSTRACT

This paper describes the results of an atmospheric tracer study in which sulfur hexafluoride (SF_6) was used to investigate the transport and dispersion of effluent from a power plant located in a coastal environment. The field study demonstrated that material emitted into an elevated stable layer at night can be transported out over the ocean, fumigated to the surface, and then be returned at ground level by the sea breeze on the next day. At night when cool stable air from the land encounters the warmer ocean convective mixing erodes the stable layer forming an internal boundary layer. When the growing boundary layer encounters an elevated plume the pollutant material, entrained at the top of the mixed layer, can be rapidly transported in ~20 min to the surface. Various expressions for the characteristic downmixing time ($\lambda = Z_i/w_*$) are developed utilizing the gradient Richardson number, the Monin-Obukhov length and turbulence intensities. Calculations using these expressions and the field data are compared with similar studies of convective mixing over the land.

1. Introduction

A major influence on pollutant dispersion and transport in coastal environments is the presence of land/sea breeze circulation systems. Unfortunately the characterization of turbulent transport is complicated by the presence of flow reversals and differing atmospheric stabilities. Since many large sources are located in shoreline environments, it is important to understand the mixing characteristics within the boundary layer. A field experiment designed to determine the fate of pollutants emitted into the offshore flow associated with a land/sea breeze circulation system, was carried out by Shair *et al.* (1981). In that study it was found that tracer material emitted into an elevated stable layer at night could be transported out over the ocean, fumigated to the surface, and then be returned at ground level by the sea breeze on the next day. The objectives of this work are to examine the vertical transport processes responsible for this rapid downmixing and to characterize the mixing rates within the internal boundary layer formed when cool air from the land is advected out over a warm ocean surface.

2. Description of field experiment

Because of the complexity of atmospheric flows, the only direct way to relate the emissions from a particular source to observed concentrations is to tag the source exhaust gases so they can be uniquely identified. Over the last few years a variety of atmospheric tracers, including sulfur hexafluoride (SF_6), fluorescent particles, halocarbons and deuterated methane, have been used in transport and diffusion studies. Sulfur hexafluoride was used in this experiment because it is gaseous, physiologically inert, chemically stable, and easily detected using electron-capture gas chromatography (Simmonds *et al.*, 1972). Drivas and Shair (1974), Lamb *et al.* (1978a,b) and Dietz and Cote (1973) have successfully demonstrated the utility of SF_6 as a tracer in large-scale field studies. Current analysis techniques have achieved detection limits of 2×10^{-13} parts SF_6 per part of air. From a practical point of view both the release techniques and sampling protocols are well established and reliable.

Each experiment was carried out by injecting the tracer gas into the number 4 stack of the Southern California Edison El Segundo power plant located on the shore of Santa Monica Bay (Fig. 1). This particular chimney is 61 m high and 4.3 m in diameter. The tracer was released at a time when the flow, at the effective stack height, was offshore. Before each experiment an initial estimate of the plume rise was determined using Briggs' formulas (Briggs, 1969; 1975) for neutral conditions. For the particular load conditions (0.57 of capacity), an exhaust gas temperature of 365 K and a gas flow rate of 230 m^3 s^{-1}, the plume rise was estimated to be 250 m. This information, together with the vertical wind distribution obtained from pibal releases, was used to establish the time to initate the tracer injection so that the material was released into the offshore flow. After the experiment a more detailed calculation,

[1] Department of Chemical Engineering.

0021-8952/81/111312-13$07.25

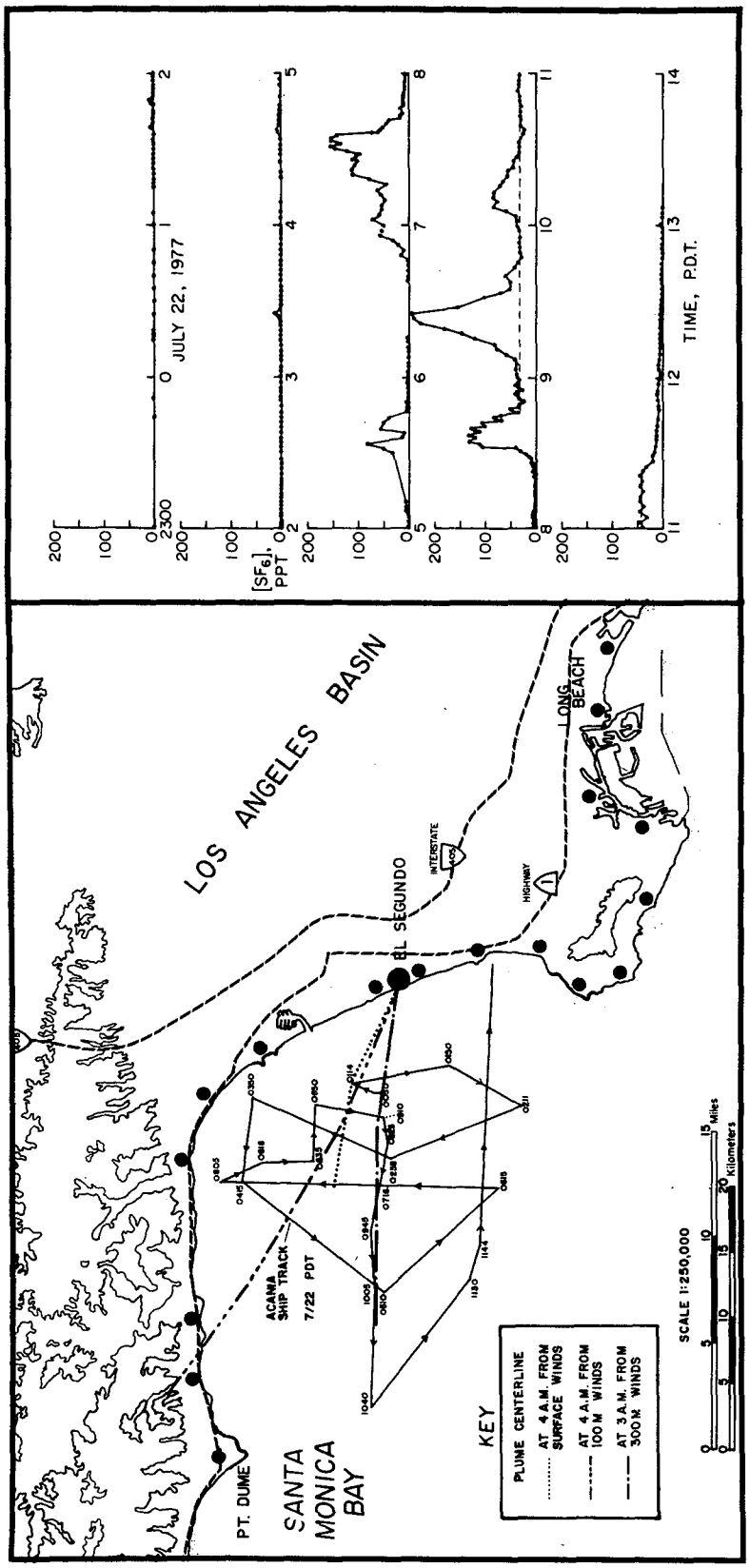

FIG. 1. Sulfur hexafluoride (SF_6) measurements made on board R/V *Acania* 22 July 1977 coordinated with ship course and possible plume trajectories derived from surface and elevated wind measurements: (●), release site; (●) onshore monitoring sites.

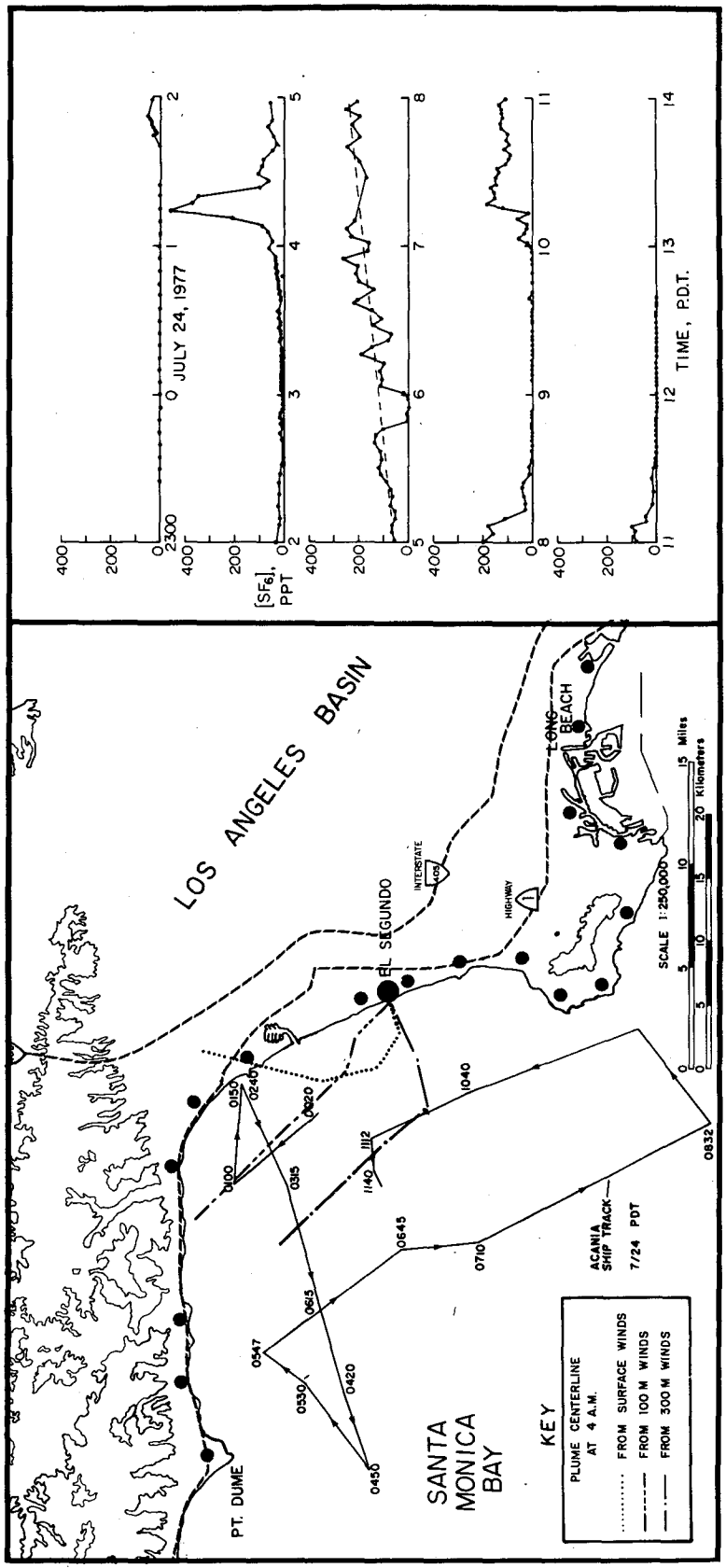

FIG. 2. Sulfur hexafluoride (SF_6) measurements made on board R/V *Acania* 24 July 1977 coordinated with ship course and possible plume trajectories derived from surface and elevated wind measurements: (●) release site; (●) onshore monitoring sites.

accounting for the actual vertical variations in wind and temperature profiles, was carried out using the Schatzmann (1979) integral plume rise model, using meteorological data from Schacher *et al.* (1978). During the first test, on 22 July 1977, 90 kg of SF_6 was released at a rate of 5.0 g s^{-1} from 0005–0500 (all times PDT). During the second test 245 kg of SF_6 were released, at a higher rate of 13.6 g s^{-1}, from 2303 on 23 July 1977 until 0400 on 24 July.

The amount and release rates for each experiment were selected so that there was sufficient material to distinguish the source from the background at the maximum sampling distance. If the total amount of tracer released during each experiment were to be uniformly distributed throughout a volume of 1600 $km^2 \times 300$ m (i.e., the area of Santa Monica Bay times the estimated plume rise above the ocean surface), then the average tracer concentration would have been 50 ppt[2], a value well above both the detection limit and normal background levels. Most of the current world background concentration of <0.5 ppt is a result of leakages from high-voltage power transformers and switching systems where SF_6 is used for corona discharge suppression.

Hourly averaged air samples were collected continuously, from 0500–1700 during each of the test days, at 29 coastal sites located from Ventura to Corona del Mar (Figs. 1 and 2). This was to observe the tracer flux across the coast during the sea breeze on the day following the nighttime release. Subsequent mass balance calculations using these measurements were able to account for virtually 100% of the material released during both experiments (Shair *et al.*, 1981). Samples were analyzed using the methodology described in Lamb *et al.* (1978a,b). In addition, grab samples were collected every 5 min on board a ship traversing Santa Monica Bay and analyzed using portable electron-capture gas chromatographs. This sampling protocol provided rapid feedback on the tracer concentrations and plume position during each experiment. The measurements taken on board the ship are shown in Figs. 1 and 2. Sampling on board the ship was started 1 h before each release so that any possible background levels could be detected. All samples were collected in 30 cm^3 plastic syringes and were analyzed within one day of each experiment. At the coastal monitoring sites battery-powered sequential samplers were used to determine the hourly averaged SF_6 concentration levels. In addition automobile sampling traverses were conducted periodically along coastal highways between 1000–1427 on 22 July and between 0235–1540 on 24 July. Grab samples were collected at 0.8–3.2 km intervals along the coastal highway between Redondo Beach and Malibu. The results from the shore measurements and automobile traverses were used by Shair *et al.* (1981) to calculate the flux of SF_6 across the coast.

The tracer experiments were carried out in collaboration with investigators from the Environmental Physics Group at the Naval Postgraduate School in Monterey, California. The research vessel *Acania* was used as a platform to collect meteorological data in the vicinity of Santa Monica Bay. The ship was equipped with a complete suite of meteorological equipment capable of multilevel measurements (4.2, 7.0 and 22.5 m above the ocean) of mean and fluctuating quantities. Since complete details of the instrumentation can be found in Houlihan *et al.* (1978) and Schacher *et al.* (1978), the material will not be repeated here. For the particular study of the mixing rates over the ocean, measurements were made of sea surface temperature T_s, air temperature T_a, humidity/dew point T_d, true wind speed u, direction θ, and temperature inversion height Z_i. The wind direction θ is particularly useful since it can be used to differentiate local (land and sea breeze) circulations. Both the wind speed and direction have been corrected to account for the ship motion. In addition, during the period 19–26 July, 14 radiosondes were released to examine the vertical temperature structure. During each tracer experiment pibals were released each hour at a site close to the release point so that the horizontal winds as a function of elevation could be determined. Observations made at the 100 and 300 m levels were used to calculate plume trajectories from the release point. Some of these results are superimposed on Figs. 1 and 2. The complete data sets describing the meteorological conditions are contained in the reports by Schacher *et al.* (1978, 1980). For convenience a summary of key information from these sources, together with the calculated virtual heat flux Q_0, is presented in Table 1.

Since the pattern of results observed on board R/V *Acania* on both days were similar it suffices to discuss the experiment conducted on 22 July. A more detailed discussion of the concentration levels measured at the coastal monitoring stations is contained in Shair *et al.* (1981). Prior to 0530 PDT, when the mixing depth was below 200 m, the ship passed under the calculated plume positions at 0100, 0325 and 0438 and no significant concentrations of SF_6 were observed. At 0530, when the ship was 6.4 km south of the plume, the first significant peak (80 ppt) was recorded at a time when the mixed layer was growing above the 200 m level. From 0600 onward all the concentration peaks at 0730, 0835 and 0925 were observed when the ship was in the vicinity of the plume and the mixed-layer height was above 200 m. From 0830 to 1130 the SF_6 exceeded 20 ppt and the ship was always within 3 km of the plume. Lower concentrations were observed when the ship

[2] Parts per trillion.

TABLE 1. Basic meterological data collected during the period 19–26 July 1977.*

Date	Time (PDT)	Humidity (%)	T_a (°C)	T_s (°C)	T_a-T_s (°C)	Q_0 (10^3 m s^{-1} K)	Date	Time (PDT)	Humidity (%)	T_a (°C)	T_s (°C)	T_a-T_s (°C)	Q_0 (10^3 m s^{-1} K)
19	0000	90	16.4	19.1	−2.75	8.7	21	0945	89	17.5	18.8	−1.26	2.8
19	0020	92	16.0	18.5	−2.53	5.6	21	1005	88	17.4	18.2	−0.72	2.1
19	0100	92	16.0	17.6	−1.61	2.4	21	1025	88	17.6	18.5	−0.38	0.8
19	0140	93	15.9	16.7	−0.80	0.7	21	1045	88	17.6	18.4	−0.80	1.6
19	1620	79	18.7	21.1	−2.39	14.9	21	1105	89	17.4	17.7	−0.33	2.1
19	1650	79	18.5	21.1	−2.57	19.4	21	1305	90	17.7	17.7	−0.05	2.2
19	1710	79	18.3	21.0	−2.72	18.8	21	1325	90	17.5	17.7	−0.24	3.0
19	1730	79	18.1	20.9	−2.77	19.4	21	1345	90	17.5	17.9	−0.40	3.0
19	2000	84	18.2	18.8	−0.59	5.8	21	1405	90	17.7	18.2	−0.54	4.6
19	2040	87	17.5	19.8	−2.26	11.8	21	1505	88	18.2	18.9	−0.68	7.9
19	2120	87	17.5	19.8	−2.26	7.3	21	1620	86	18.3	18.8	−0.47	6.6
19	2140	87	17.6	19.9	−2.33	7.5	21	1720	85	18.0	18.7	−0.69	6.4
19	2200	87	17.6	19.8	−2.20	8.9	21	1945	79	18.6	19.9	−1.30	10.4
							21	2030	85	18.2	19.8	−1.66	7.5
20	0700	86	17.0	18.7	−1.67	9.9	21	2110	84	18.3	19.7	−1.35	3.4
20	0740	86	17.3	19.2	−1.93	8.5	21	2130	85	18.3	19.5	−1.21	3.8
20	0900	85	17.8	19.3	−1.46	4.6							
20	0920	85	17.9	19.3	−1.42	4.4	22	0550	93	17.1	17.3	−0.19	0.5
20	1240	78	19.0	20.2	−1.20	5.2	22	0610	94	16.9	17.2	−0.34	0.7
20	1300	79	19.0	19.8	−0.78	3.2	22	0710	96	16.5	17.3	−0.77	0.5
20	1320	88	19.0	19.7	−0.63	2.3	22	0730	97	16.6	17.3	−0.68	0.4
20	1800	84	18.8	18.2	0.56	−3.9	22	0750	97	16.5	17.3	−0.76	0.5
20	1900	83	18.3	17.8	0.48	−4.3	22	0810	97	16.7	17.3	−0.57	0.3
20	1920	84	18.4	17.7	0.65	−6.4	22	0830	96	16.6	17.3	−0.72	2.1
20	1940	84	18.3	18.4	−0.12	2.5	22	0910	97	16.5	17.3	−0.78	1.4
20	2000	85	18.2	18.3	−0.09	2.1	22	0930	97	16.6	17.3	−0.71	0.8
20	2020	86	17.7	18.3	−0.56	3.7	22	1030	96	17.1	18.5	−1.46	4.6
20	2040	87	17.9	18.3	−0.45	2.5	22	1050	94	17.5	18.6	−1.09	1.4
20	2120	88	17.8	18.2	−0.41	2.3							
20	2140	89	17.7	18.2	−0.53	2.8	23	1440	87	19.2	18.2	0.92	−1.4
20	2220	90	17.6	19.0	−1.38	4.8	23	1505	85	19.5	18.7	0.76	−2.9
20	2230	91	17.6	18.4	−0.83	2.7	23	1645	83	19.9	20.4	−0.43	5.1
20	2300	91	17.2	18.2	−1.00	2.9	23	1725	85	19.1	19.2	−0.08	1.9
							23	1745	87	18.8	19.1	−0.28	1.2
21	0000	94	16.6	17.2	−0.63	2.5	23	2340	90	18.5	18.0	0.53	−0.5
21	0040	94	16.2	16.9	−0.70	2.5							
21	0100	93	15.9	16.6	−0.72	2.0	24	0040	91	19.1	18.6	0.50	−0.7
21	0405	98	16.2	17.7	−1.46	6.3	24	0100	90	19.0	18.6	0.39	−0.5
21	0425	97	16.4	18.1	−1.65	6.2	24	0120	90	19.0	18.7	0.28	−0.3
21	0445	96	16.8	18.4	−1.57	6.0	24	0240	87	19.0	18.7	0.25	−0.3
21	0505	94	17.1	18.4	−1.33	4.5	24	0300	86	19.0	18.7	0.28	−0.3
21	0545	91	17.4	18.2	−0.81	2.2	24	0420	88	18.8	18.7	0.06	0.0
21	0605	89	17.4	18.3	−0.84	0.7	24	1000	78	19.3	19.2	0.06	0.5
21	0645	89	17.3	18.3	−0.96	2.0							
21	0705	89	17.3	18.2	−0.86	2.4	25	2220	83	19.3	17.7	1.57	−8.8
21	0845	91	17.7	19.0	−1.31	6.4	25	2320	84	19.1	17.9	1.27	−7.1
21	0905	89	17.8	18.9	−1.14	3.9	26	0420	90	18.6	18.1	0.49	−0.2

* Source: Schacher *et al.* (1980).

and the plume separation increased to more than 15 km. The only major difference between the two tests was the increased wind speeds and mixing heights on 23–24 July. While this, together with the wind shear, enhanced the horizontal dispersion of SF_6 there were no significant differences in the observed vertical mixing rates.

Although the power plant effluent was emitted well above the surface into an elevated stable layer where vertical mixing could be expected to be quite small, large amounts of tracer suddenly appeared at the sampling sites close to the ocean surface. The remaining sections of this work are devoted to a discussion of the reasons for the rapid transport of tracer material to the surface.

3. Vertical mixing over the ocean

The problem of dispersion and transport near coastlines and large lakes has received considerable attention in the literature (See, e.g., Lyons, 1975; Businger, 1975; Misra, 1980; Raynor *et al.*, 1980 Orgill, 1981). The purpose of this section is to examine the results from prior observations applicable to the present field experiment, since few, if any, studies have been made of convective activity over the ocean at night. Since the ocean temperatures during the experiments were greater than that of the air, it can be seen that the conditions are similar to those observed over the land during the day.

Under the action of buoyancy forces induced by

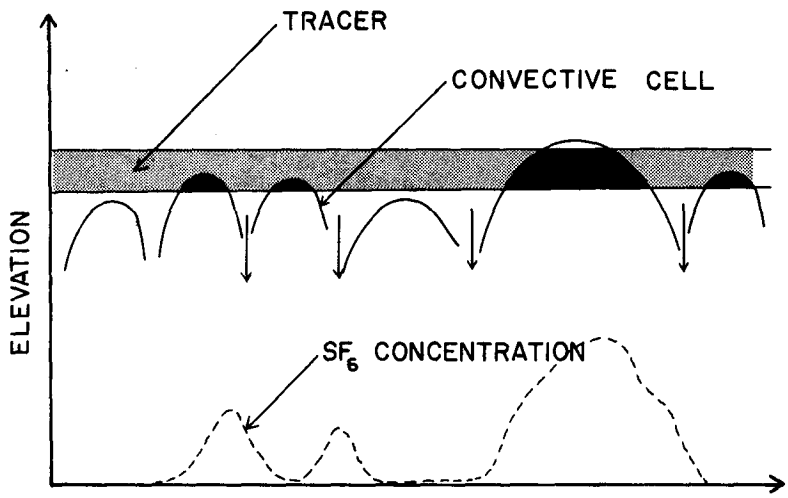

FIG. 3. Intermittent entrainment of tracer material by convective cells.

surface heating, parcels of warm air, displaced by mechanical turbulence, rise all the way through the mixed layer and impinge at the inversion base. To compensate for these vertical motions, zones of sinking air fill the spaces between rising air parcels. Close to the top of the mixed layer the net flux is directed downward. Adiabatic transport of air through the capping inversion would produce the negative flux, which in turn suggests a mechanism for substantial entrainment of air and tracer material into the mixed layer from above (Ball, 1960; Kaimal *et al.*, 1976; Deardorff *et al.*, 1980). The regions of upward flux are obviously thermals which originate near the surface shear layer and the transport is thus occurring over a scale Z_i.

The updraft regions in the thermals resembles the three-dimensional convection patterns observed by Frisch *et al.* (1975) with dual-Doppler radar. Kaimal *et al.* (1976) suggested that the rising air spreads out laterally as it reaches the inversion base, producing a domelike depression at the interface, and returns as a downdraft along the "side wall" of the thermal. These structures can be observed with acoustic sounders and radars. Arnold *et al.* (1975) found that domelike structures are colocated with the thermals detected simultaneously by an acoustic sounder. The strong returns from the side walls indicate the presence of entrained air from the inversion. The inverted U structures in the vertical section and the doughnut-shaped patterns in plan views observed by Hardy and Ottersten (1969), Konrad (1970), Arnold and Rowland (1976) and Agee and Chen (1973) in radar returns indicate the presence of convective cells.

Arnold and Rowland (1976) conclude that most of the entrainment takes place along the top of the dome. Here either the Kelvin-Helmholtz instability or wavelike overturning of the dome structures could provide the mechanism for entrainment. This process is illustrated in Fig. 3 where the tops of the convective cells can rise to the elevation of the SF_6. Entrainment of this material and its subsequent transport to the surface lead to the large concentration increases. Areas of low concentration would then result when the ship went beyond the bounds of the cloud or when the convective cells did not reach the height of the tracer. A detailed examination of the mechanism of entrainment and mixed-layer growth is beyond the scope of this work and for details the reader is referred to Stull (1973), Venkatram (1976), Zeman and Tennekes (1977), Heidt (1977) and Deardorff (1978). Convective entrainment has been studied in the laboratory by Willis and Deardorff (1976a), Manins (1977) and Deardorff *et al.* (1980). The characteristic separation distance of the thermals given by Kaimal *et al.* (1976) is $1.3-1.4Z_i$ with the diameter-to-depth ratio for the Rayleigh cells being of the order of 40:1 (Agee and Chen, 1973).

With this background it is now possible to advance an explanation of the findings from the tracer experiments. When the cool stable air from the land encounters the warmer ocean surface, convective mixing begins to erode the overlying stable layer forming an internal boundary layer (Fig. 4). (The growth of this layer as a function of distance from the shore can be seen in the acoustic sounder traces.) Convective mixing in the surface layer entrains air from the stable layer aloft causing the inversion base to rise from the surface. Heating of the mixed layer is due to the combined effects of an upward heat flux from the ocean and a downward flux from the warmer air in the inversion. Continued growth of the mixed layer ultimately leads to a situa-

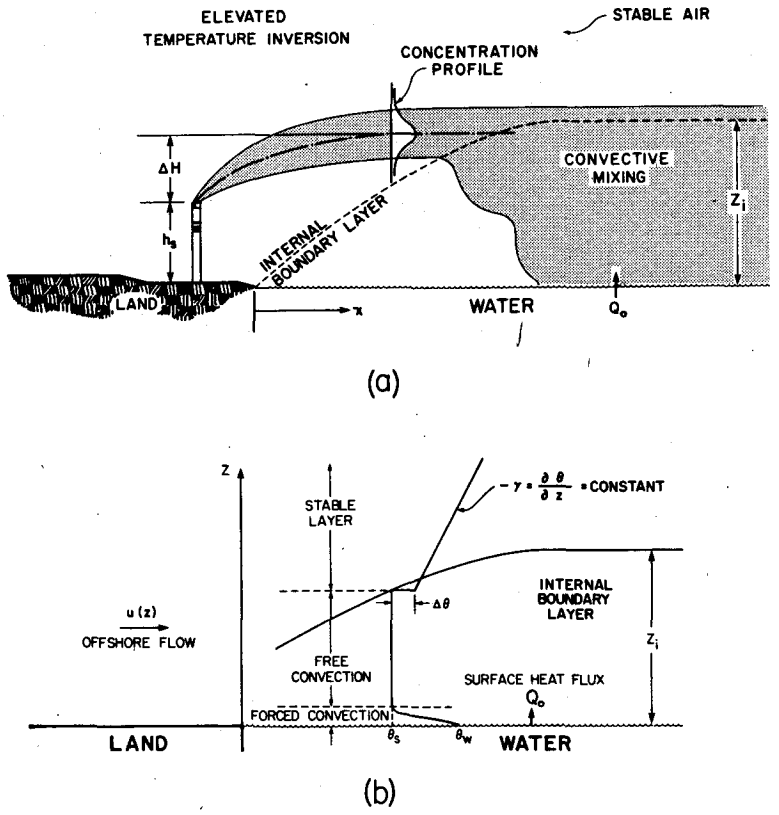

FIG. 4. Schematic representation of (a) fumigation process and (b) notation for mixing model.

tion where the internal boundary layer intercepts the elevated plume and the tracer materials. Since below the inversion base the mixing is rapid, the entrained SF_6 is quickly transported to the surface. Except for the strength of the convective mixing, the conditions of the experiment are similar to those that occur over the land during the day. Subsequent sections of this work are devoted to an estimate of the rate at which the tracer material is transported to the surface.

4. Mixing times under convective conditions

Under convective conditions a variety of interacting processes are involved in the mixing within the boundary layer. The relative role of buoyancy $\overline{w'T_v'}$, in comparison with the transfer of energy from the mean motion $\overline{u'w'}\partial\bar{u}/\partial z$, can be expressed in terms of the flux Richardson number R_f (Monin and Yaglom, 1971; Kraus, 1972), as

$$R_f = \frac{\frac{g}{T}\overline{T_v'w'}}{\overline{u'w'}\frac{\partial\bar{u}}{\partial z}}, \quad (1)$$

where T_v is the virtual temperature. A more commonly used expression is the gradient Richardson number Ri

$$\mathrm{Ri} = \frac{g\left(\frac{\partial\bar{T}_v}{\partial z} + \Gamma\right)}{T_v\left(\frac{\partial\bar{u}}{\partial z}\right)^2} = \frac{g}{\theta_v}\frac{\frac{\partial\bar{\theta}_v}{\partial z}}{\left(\frac{\partial\bar{u}}{\partial z}\right)^2} = \frac{N^2}{\left(\frac{\partial\bar{u}}{\partial z}\right)^2}, \quad (2)$$

where N is the Brunt-Väisälä frequency, θ_v the potential temperature, and Γ the adiabatic lapse rate. The relationship between R_f and the more easily measured Richardson number Ri is simply $R_f = \alpha\,\mathrm{Ri}$, where α is the ratio of the turbulent eddy diffusion coefficients for heat and momentum. Under a spatial homogeneity assumption temporal changes in the total mean kinetic energy are negligible if synoptic and mesoscale forces driving the boundary layer vary slowly (Caughey *et al.*, 1978). In particular, if the time scales for the large-scale processes are long compared to the time required for the boundary layer to adjust then the rate of change of turbulent kinetic energy per unit mass is negligible. If the contribution from the flux divergence term in the energy equation is small,

TABLE 2. Additional data and calculated results for period 19–26 July 1977.*

Date	Time (PDT)	u (m s^{-1})	θ (K)	Z_i/L	u_* (m s^{-1})	T_* (K)	Z_i (m)	w_* (m s^{-1})	λ (min)
19	0000	1.5	283	−4.840	0.060	−0.117	280	0.436	11
19	0020	1.0	308	−8.206	0.044	−0.104	330	0.397	14
19	0100	0.5	317	−18.190	0.025	−0.075	320	0.296	18
19	0140	0.3	11	−29.206	0.014	−0.035	190	0.166	19
19	1620	3.1	294	−1.125	0.112	−0.077	470	0.585	13
19	1650	3.9	272	−0.754	0.142	−0.085	500	0.663	13
19	1710	3.6	275	−0.929	0.132	−0.093	490	0.659	12
19	1730	3.7	285	−0.889	0.136	−0.096	480	0.665	12
19	2000	4.4	277	−0.216	0.156	−0.023	500	0.477	17
19	2040	3.0	280	−1.134	0.108	−0.082	540	0.597	15
19	2120	1.5	5	−4.174	0.060	−0.092	590	0.525	19
19	2140	1.5	318	−4.291	0.060	−0.096	600	0.534	19
20	0700	3.6	285	−0.542	0.129	−0.051	160	0.369	7
20	0740	2.5	260	−1.433	0.089	−0.068	230	0.400	10
20	0900	1.5	250	−2.852	0.058	−0.053	160	0.290	9
20	0920	1.5	250	−2.502	0.058	−0.044	180	0.286	10
20	1240	2.0	195	−1.645	0.071	−0.036	360	0.385	16
20	1300	1.8	206	−1.459	0.064	−0.020	360	0.332	18
20	1320	2.0	220	−0.773	0.069	−0.013	280	0.264	18
20	1800	7.2	186	0.045	0.259	0.036	80		
20	1900	6.2	275	0.079	0.213	0.042	140		
20	1920	7.2	250	0.058	0.257	0.041	160		
20	1940	7.2	270	−0.004	0.267	0.013	260	0.069	
20	2000	5.7	270	−0.024	0.203	0.007	280	0.228	20
20	2020	5.1	270	−0.056	0.183	−0.001	240	0.273	15
20	2040	3.6	280	−0.158	0.123	−0.005	200	0.248	13
20	2120	3.6	270	−0.150	0.123	−0.005	240	0.258	15
20	2140	3.5	260	−0.186	0.120	−0.009	240	0.272	15
20	2220	2.0	280	−1.606	0.071	−0.048	340	0.378	15
20	2230	2.0	290	−0.931	0.069	−0.023	340	0.305	19
20	2300	2.3	302	−0.356	0.080	−0.030	300	0.328	15
21	0000	2.6	255	−0.470	0.087	−0.020	280	0.288	16
21	0040	2.6	259	−0.441	0.087	−0.019	310	0.290	18
21	0100	1.8	305	−0.876	0.063	−0.019	200	0.227	15
21	0120	1.0	141	−1.656	0.039	−0.014	270	0.193	23
21	0405	3.1	85	−0.595	0.108	−0.048	240	0.370	11
21	0425	2.5	125	−1.106	0.088	−0.058	320	0.406	13
21	0445	2.6	142	−0.994	0.090	−0.054	380	0.425	15
21	0505	2.1	125	−1.443	0.073	−0.049	360	0.380	16
21	0545	1.5	160	−1.497	0.056	−0.025	455	0.319	24
21	0605	0.2	160	−43.572	0.012	−0.031	460	0.213	36
21	0645	1.0	100	−3.625	0.040	−0.030	480	0.310	26
21	0705	1.5	100	−1.691	0.055	−0.026	460	0.326	23
21	0845	3.1	95	−0.583	0.108	−0.040	475	0.457	17
21	0905	2.1	91	−1.158	0.072	−0.032	430	0.368	19
21	0945	1.0	129	−4.270	0.041	−0.040	360	0.310	19
21	1005	1.5	135	−1.164	0.055	−0.014	310	0.252	21
21	1025	0.2	200	−39.449	0.012	−0.024	300	0.176	28
21	1045	0.8	235	−3.474	0.033	−0.015	280	0.212	22
21	1105	3.6	270	−0.035	0.120	0.006	260	0.143	30
21	1305	7.2	258	0.006	0.264	0.012	180		
21	1325	7.0	260	0.000	0.256	0.009	210		
21	1345	6.5	280	−0.003	0.237	0.008	200	0.079	42
21	1405	6.7	285	−0.020	0.246	0.000	200	0.244	14
21	1505	6.5	280	−0.045	0.240	−0.007	200	0.318	10
21	1620	7.0	260	−0.021	0.260	0.003	200	0.258	13
21	1720	5.5	270	−0.058	0.198	−0.003	120	0.239	8
21	1945	4.0	250	−0.397	0.144	−0.038	250	0.428	10
21	2030	2.5	225	−1.328	0.089	−0.059	150	0.336	7
21	2110	1.0	220	−5.585	0.042	−0.053	300	0.325	15
21	2130	1.5	220	−2.618	0.056	−0.043	310	0.341	15
22	0550	2.0	130	−0.209	0.065	0.000	205	0.143	24
22	0610	1.5	130	−0.550	0.053	−0.006	220	0.169	22
22	0710	0.2	140	−35.247	0.012	−0.030	240	0.157	26

TABLE 2. (*Continued*)

Date	Time (PDT)	u (m s^{-1})	θ (K)	Z_i/L	u_* (m s^{-1})	T_* (K)	Z_i (m)	w_* (m s^{-1})	λ (min)
22	0730	0.2	120	−29.493	0.012	−0.024	240	0.144	28
22	0750	0.2	140	−32.846	0.012	−0.028	240	0.152	26
22	0810	0.2	150	−21.592	0.011	−0.015	245	0.126	33
22	0830	2.1	180	−0.631	0.070	−0.018	230	0.238	16
22	0910	1.0	307	−2.365	0.040	−0.024	210	0.205	17
22	0930	0.5	270	−6.285	0.023	−0.020	220	0.165	22
22	1010	2.6	260	−0.763	0.089	−0.040	240	0.330	12
22	1030	2.0	250	−1.369	0.071	−0.045	260	0.326	13
22	1050	0.5	305	−10.055	0.024	−0.033	260	0.213	20
23	1440	2.5	250	1.332	0.050	0.031	280		
23	1505	3.9	215	0.285	0.114	0.039	310		
23	1645	4.6	275	−0.086	0.163	0.001	320	0.307	17
23	1725	4.9	262	−0.011	0.170	0.012	355	0.112	
23	1745	2.1	244	−0.268	0.068	0.004	350	0.188	31
23	2340	1.7	260	1.943	0.029	0.017	500		
24	0040	2.1	281	0.527	0.052	0.017	155		
24	0100	1.8	270	0.776	0.043	0.017	120		
24	0120	1.5	236	0.767	0.037	0.014	170		
24	0240	1.7	140	0.381	0.046	0.016	120		
24	0300	1.5	136	0.455	0.041	0.016	160		
24	0420	1.0	210	0.044	0.032	0.011	140		
24	1000	1.0	269	−0.091	0.034	0.021	165		
25	2220	5.0	270	0.340	0.150	0.068	160		
25	2320	5.0	280	0.231	0.157	0.054	160		
26	0420	1.4	340	3.147	0.019	0.012	90		

* Source: Schacher *et al.* (1980).

then, with the above assumptions, the turbulent kinetic energy equation reduces to

$$-\overline{u'w'}\frac{\partial \bar{u}}{\partial z}(1 - R_f) - \epsilon = 0, \tag{3}$$

where ϵ is the dissipation or the rate of conversion of kinetic into internal energy by the viscous forces in the smallest eddies. Since $\epsilon > 0$ and $-\overline{u'w'}\partial\bar{u}/\partial z$ is practically always greater than zero, stationary, undamped turbulence is possible only if $R_f < 1$. This result is often used as an approximate criterion for defining the transition to turbulence in a stratified medium. For the purpose of analyzing the experimental results within this framework it is useful to identify the appropriate length and velocity scales. A key scaling parameter is the Monin-Obukhov length L defined by

$$\frac{1}{L} = -\frac{kgQ_0}{u_*^3 T} = -\frac{kg}{u_*^3 T}\left(Q + 0.61\frac{TM_0}{\rho}\right) = \frac{1}{L_T} + \frac{1}{L_q}, \tag{4}$$

where $Q_0 = (\overline{T_v'w'})_0$ is the virtual surface heat flux that accounts for the influence of humidity fluctuations on buoyancy, k the von Kármán constant, $u_*^2 = -\overline{u'w'}$ the friction velocity, and L_T and L_q are the Monin-Obukhov lengths calculated from the surface heat and evaporative fluxes. Physically, L is the height at which the two production terms are approximately of equal magnitude. One of the major differences in examining conditions over the ocean or other large bodies of water is that the density stratification is controlled not only by the surface heat flux but also by the water vapor flux. The measurements made by McBean and MacPherson (1975) over Lake Ontario indicate that there can be a significant difference between L_q and L_T, that in turn have a major influence on L.

Above the surface layer a more appropriate length scale for the eddies is the mixed layer depth Z_i. While there is some controversy associated with a formal definition of Z_i, in this work it is defined as the elevation of the lowest inversion base. The studies of Deardorff (1972) and Deardorff *et al.* (1980) indicate that this is an appropriate boundary layer height for momentum and heat. Under convective conditions the appropriate velocity scale, above the surface layer, is given by

$$w_* = \left(\frac{g}{T}Z_iQ_0\right)^{1/3} = \left[\frac{g}{T}Z_i(\overline{w'T_v'})_0\right]^{1/3} = \left(-\frac{1}{k}\frac{Z_i}{L}\right)^{1/3}u_*. \tag{5}$$

The characteristic time scale under convective conditions is then given by $\lambda = Z_i/w_*$. Willis and Deardorff (1976b) have shown that material released instantaneously at the surface becomes nearly well mixed within a travel time of $\sim 3\lambda$. In the field experiment the tracer material was "released" at the top of the mixed layer. Apart from the small contribution due to mechanical mixing the characteristic mixing time can be expected to be similar to that for a surface release. The reason for this is that the effective aerodynamic roughness of the ocean is very small.

There are a variety of means of estimating the fluxes needed to evaluate the above expressions. Three of the more common techniques are 1) the profile or gradient method, 2) the variance budget or dissipation technique, 3) and bulk aerodynamic calculations using air-sea differences. Schacher *et al.* (1978, 1980) employed the latter approach in reducing the meteorological data from the field experiment. A detailed discussion of these and other procedures is presented in Busch (1977). The key results from Schacher *et al.* (1978, 1980) are summarized in Table 2. In particular the frequency distribution of convective mixing times observed during the period 19–23 July is shown in Fig. 5 together with a similar distribution for daytime conditions over the land. The characteristic mixing times for both experiments were very similar. The influence of a much larger surface heat flux during the day is readily apparent.

In the surface layer, the velocity distribution can be expressed in terms of Monin-Obukhov similarity theory as

$$\frac{\partial \bar{u}}{\partial z} = \frac{u_*}{kz}\phi_m\left(\frac{z}{L}\right), \tag{6}$$

where ϕ_m is an experimentally determined function that corrects for the effects of buoyancy on turbulence. Businger *et al.* (1971) have constructed expressions for momentum ϕ_m and heat ϕ_h from an analysis of field data. For unstable conditions $z/L < 0$ the formulas are given by

$$\phi_m\left(\frac{z}{L}\right) = \left[1 - 15\left(\frac{z}{L}\right)\right]^{-1/4}, \tag{7}$$

$$\phi_h^2\left(\frac{z}{L}\right) = \phi_m\left(\frac{z}{L}\right). \tag{8}$$

These results, together with (3), the definition of u_* and the relation $\mathrm{Ri} = \alpha R_f$, can combined to give

$$u_*^3 = \frac{kz}{(1 - \alpha\,\mathrm{Ri})\phi_m\left(\frac{z}{L}\right)}. \tag{9}$$

The characteristic mixing time τ_m can be defined

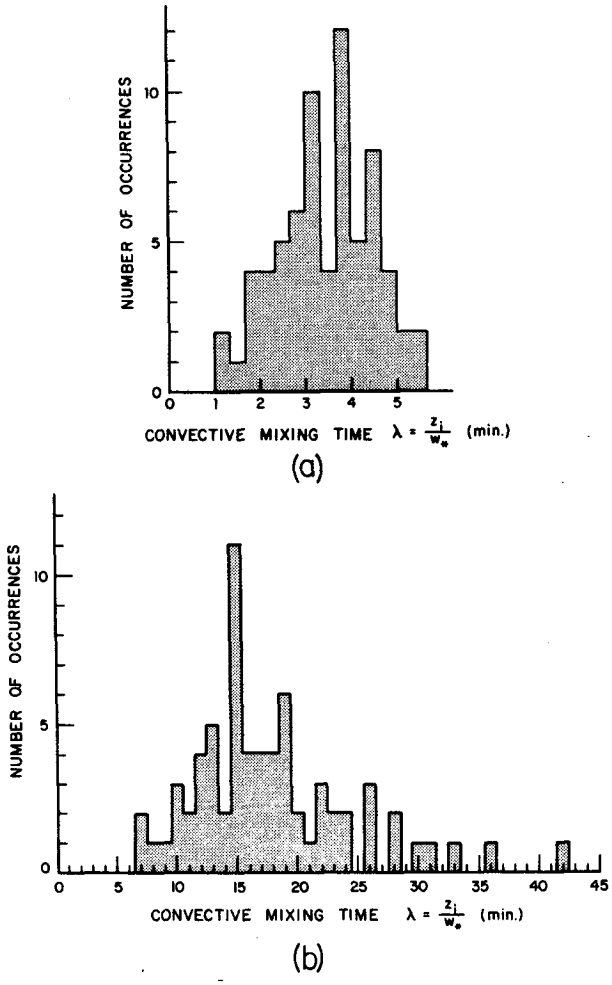

FIG. 5. Distribution of convective mixing times for (a) daytime conditions over land (source, Smith *et al.*, 1976) and (b) nighttime conditions over ocean.

in terms of the convective time scale λ as $\tau_m = 3\lambda = 3Z_i/w_*$. Using (5), and the expression $\phi_m R_f = z/L$, Eq. (9) can be manipulated to give an estimate of the mixing time in terms of the measured dissipation rate and gradient Richardson number Ri:

$$\tau_m = 3\left[\frac{Z_i^2}{\epsilon}\left(1 - \frac{1}{\alpha\,\mathrm{Ri}}\right)\right]^{1/3}. \tag{10}$$

For near-neutral conditions, Businger *et al.* (1971) determined that $\alpha = 1.35$; thus a simple upper bound on (10) is $\tau_m \approx 3[-Z_i^2/\epsilon\,\mathrm{Ri}]^{1/3}$. For unstable conditions when $|\mathrm{Ri}| \gg 1$, a lower bound is given by $\phi_m = 3[Z_i^2/\epsilon]^{1/3}$. Using the data tabulated in Appendix B of Schacher *et al.* (1978) the limits on the convective mixing times can be calculated and are shown in Table 3 for the experiment conducted on 22 July. The important result from the tracer experiments is that the calculated mixing rates using

TABLE 3. Convective mixing times based on turbulence intensities for 22 July 1977.

Date	Time (PDT)	Z_i/L	u_* (m s^{-1})	Z_i (m)	Ri	ϵ (10^{-4} m s^{-3})	$\left[\frac{Z_i^2}{\epsilon}\right]^{1/3}$ (min)	$\left[-\frac{Z_i^2}{\epsilon\,\mathrm{Ri}}\right]^{1/3}$ (min)
22	0550	−0.209	0.065	205	−0.04	1.8	10	30
22	0610	−0.550	0.053	220	−0.09	3.6	8	19
22	0710	−35.247	0.012	240	−0.16	3.6	9	17
22	0730	−29.493	0.012	240	−0.08	4.0	9	20
22	0750	−32.846	0.012	240	−0.18	2.9	10	17
22	0810	−21.592	0.011	245	−0.21	5.1	8	14
22	0830	−0.631	0.070	230	−0.10	4.6	8	17
22	0910	−2.365	0.040	210	−0.02	7.1	7	24
22	0930	−6.285	0.023	220	−0.03	7.3	7	22

either the bulk or dissipation methods produces results consistent with the observed fumigation times. The rapid concentration increases were measured during times when the ship was beneath the plume and the mixed layer height exceeded 200 m.

5. Eddy diffusion coefficients

A basic problem with modeling convectively driven flows is that the turbulent mixing is no longer described by local concentration gradients. Nevertheless, there are some circumstances in which it is desirable to parameterize the diffusive fluxes by a K-theory model. The objective of this section is to present a simple formulation that produces transport times consistent with observed fumigation rates. Some recent work by Crane *et al.* (1977) and McRae *et al.* (1981) indicates that vertical eddy diffusivity profiles for unstable conditions can be scaled by a single profile of the form

$$K_{zz} = w_* Z_i f\left(\frac{z}{Z_i}\right). \tag{11}$$

Lamb *et al.* (1975) derived an expression for f using the numerical turbulence model of Deardorff (1970). The profile adopted by McRae *et al.* (1981) is given by

$$\frac{K_{zz}}{w_* Z_i} = \begin{cases} 2.5\left(\frac{kz}{Z_i}\right)^{4/3}\left[1 - 15\left(\frac{z}{L}\right)\right]^{1/4}, & 0 < \frac{z}{Z_i} \leq 0.05 \\ 0.021 + 0.408\left(\frac{z}{Z_i}\right) + 1.352\left(\frac{z}{Z_i}\right)^2 - 4.096\left(\frac{z}{Z_i}\right)^3 + 2.560\left(\frac{z}{Z_i}\right)^4, & 0.05 < \frac{z}{Z_i} \leq 0.6 \\ 0.2 \exp\left[6 - 10\left(\frac{z}{Z_i}\right)\right], & 0.6 < \frac{z}{Z_i} \leq 1.1 \\ 0.0013, & \frac{z}{Z_i} > 1.1. \end{cases} \tag{12}$$

As can be seen from Fig. 6 the maximum value of the diffusivity occurs when $z/Z_i \approx 0.5$ and has a magnitude $\sim 0.21 w_* Z_i$. For typical conditions this corresponds to a diffusion time, defined by Z_i^2/K_{zz}, of $\sim 5Z_i/w_*$ that is quite consistent with the bounds shown in Tables 2 and 3.

6. Conclusions

There are a number of important findings from the tracer study that are of direct relevance to air pollution studies, first of which is that close to the shoreline different stabilities can exist above the land and water surfaces. Under these conditions atmospheric stability cannot be easily determined in terms of conventional classifications. A second finding is that the presence of convective activity can cause downmixing or fumigation of material that can return the next day as a significant increment to the onshore ground-level concentration. The process by which this occurs is as follows. During the night, cool stable air is advected out over the ocean. When this air encounters the warmer ocean surface convective mixing begins to erode the stable layer. Once the internal boundary layer has grown to the height of the plume the tracer material, entrained at the top of the mixed layer, is rapidly fumigated to the surface. The characteristic mixing time, inferred from the concentration records, is consistent with an estimate based on the convective time scale $\lambda = Z_i/w_*$ that, for the conditions of the experiment, was ~20 min.

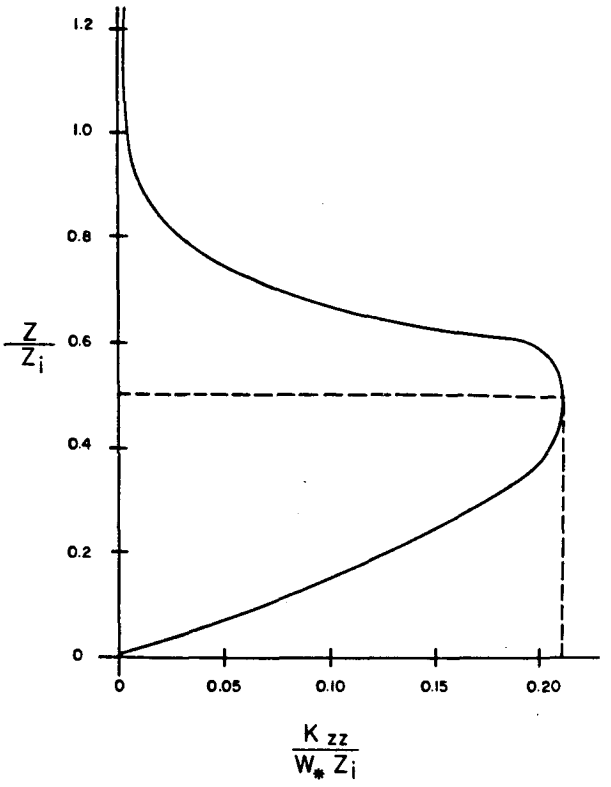

FIG. 6. Vertical turbulent diffusivity profile for unstable conditions (source, McRae *et al.*, 1981).

Understanding of these mixing processes and convective activity over the ocean will improve the ability to predict atmospheric dispersion in coastline environments.

Acknowledgments. This work was supported by the California Air Resources Board under contracts A5-187-30, A5-046-87 and A7-187-30. The assistance of Gordon Schacher of the Naval Postgraduate School, who supplied descriptions of data reduction procedures and measurement equipment, and Charles Bennett of the California Air Resources Board is appreciated.

REFERENCES

Agee, E. M., and T. S. Chen, 1973: A model for investigating eddy viscosity effects on mesoscale convection. *J. Atmos. Sci.*, **30**, 180–189.

Arnold, A., and J. R. Rowland, 1976: Fine scale observation of free convection in the atmospheric boundary layer. *Preprints Third Symp. Atmospheric Turbulence Diffusion and Air Quality*, Raleigh, Amer. Meteor. Soc., 1–8.

——, T. G. Konrad, J. H. Richter, D. R. Jensen and V. R. Noonkester, 1975: Simultaneous observation of clear air convection by a pulse radar, an FM-CW radar, an acoustic sounder and an instrumented aircraft. *Preprints 16th Radar Meteorology Conf.*, Houston, Amer. Meteor. Soc., 290–295.

Ball, F. K., 1960: Control of inversion height by surface heating. *Quart. J. Roy. Meteor. Soc.*, **86**, 483–494.

Briggs, G. A., 1969: *Plume Rise.* Atomic Energy Commission Review Series, 81 pp. [NTIS TID-25075].

——, 1975: Plume rise predictions. *Lectures on Air Pollution and Environmental Impact Analysis*, D. A. Haugen, Ed. Amer. Meteor. Soc., 59–111.

Busch, N. E., 1977: Fluxes in the surface boundary layers over the sea. *Proceedings of a NATO Advanced Study Institute, Urbino, Italy, (1975)*, Pergamon Press, 72–91.

Businger, J. A., 1975: Interactions of sea and atmosphere. *Rev. Geophys. Space Phys.*, **13**, 720–726, 817–822.

——, J. C. Wyngaard, Y. Izumi and E. F. Bradley, 1971: Flux-profile relationship in the atmospheric surface layer. *J. Atmos. Sci.*, **28**, 181–189.

Caughey, S. J., B. A. Crease, D. N. Asmakopoulos and R. S. Cole, 1978: Quantitative bistatic acoustic sounding of atmospheric boundary layer. *Quart. J. Roy. Meteor. Soc.*, **104**, 147–161.

Crane, G., H. A. Panofsky and O. Zeman, 1977: A model for dispersion from area sources in convective turbulence. *Atmos. Environ.*, **11**, 893–900.

Deardorff, J. W., 1970: A three-dimensional numerical investigation of the idealized planetary boundary layer. *Geophys. Fluid Dyn.*, **1**, 377–410.

——, 1972: Numerical investigation of neutral and unstable planetary boundary layers. *J. Atmos. Sci.*, **29**, 91–115.

——, 1978: Prediction of convective mixed-layer entrainment for realistic capping inversion structure. *J. Atmos. Sci.*, **36**, 424–436.

——, G. E. Willis and B. H. Stockton, 1980: Laboratory studies of the entrainment zone of a convectively mixed layer. *J. Fluid Mech.*, **100**, 41–64.

Dietz, R. N., and E. A. Coté, 1973: Tracing atmospheric pollutants by gas chromatographic determination of sulfur hexafluoride. *Environ. Sci. Tech.*, **7**, 338–342.

Drivas, P. J., and F. H. Shair, 1974: A tracer study of pollutant transport and dispersion in the Los Angeles area. *Atmos. Environ.*, **8**, 1155–1163.

Frisch, A. S., R. B. Chadwick, W. R. Moninger and J. M. Young, 1975: Observation of boundary layer convection cells measured by dual-Doppler radar and echosounder and by microbarograph array. *Bound.-Layer Meteor.*, **3**, 199–226.

Hardy, K. R., and H. Ottersten, 1969: Radar investigation of convective patterns in the clear atmosphere. *J. Atmos. Sci.*, **26**, 666–672.

Heidt, F. D., 1977: The growth of the mixed layer in a stratified fluid due to penetrative convection. *Bound.-Layer Meteor.*, **12**, 439–461.

Houlihan, T. M., K. L. Davidson, C. W. Fairall and G. E. Schacher, 1978: Experimental aspects of a shipboard system used in investigation of overwater turbulence and profile relationships. Naval Postgraduate School Rep. No. NPS61-78-001, 254 pp.

Kaimal, J. C., J. C. Wyngaard, D. A. Haugen, O. H. Coté and Y. Izumi, 1976: Turbulence structure in the convective boundary layer. *J. Atmos. Sci.*, **33**, 2152–2169.

Kraus, E. B., 1972: *Atmosphere-Ocean Interaction.* Clarendon Press, 275 pp.

Konrad, T. G., 1970: The dynamics of the convective process in clear air as seen by radar. *J. Atmos. Sci.*, **27**, 1138–1147.

Lamb, B. K., A. Lorenzen and F. H. Shair, 1978a: Atmospheric dispersion within coastal regions—Part I. Tracer study of power plant emissions from the Oxnard Plain. *Atmos. Environ.*, **12**, 2089–2100.

——, F. H. Shair and T. B. Smith, 1978b: Atmospheric dispersion within coastal regions—Part II. Tracer study of industrial emissions in the California Delta region. *Atmos. Environ.*, **12**, 2101–2118.

Lamb, R. G., H. W. Chen and J. H. Seinfeld, 1975: Numerico-empirical analysis of atmospheric diffusion theories. *J. Atmos. Sci.*, **32**, 1754–1807.

Lyons, W. A., 1975: Turbulent diffusion and pollutant transport in shoreline environments. *Lectures on Air Pollution and Environmental Impact Analysis*, D. A. Haugen, Ed., Amer. Meteor. Soc., 59–111.

Manins, P. C., 1977: Fumigation and a laboratory experiment. *Weather*, June, 221–228.

McBean, G. A., and J. I. MacPherson, 1975: Turbulence above Lake Ontario: velocity and scalar statistics. *Bound.-Layer Meteor.*, **10**, 181–197.

McRae, G. J., W. R. Goodin and J. H. Seinfeld, 1981: Development of a second generation mathematical model for urban air pollution: I Model formulation. *Atmos. Environ.*, (in press).

Misra, P. K., 1980: Dispersion from tall stacks into a shore line environment. *Atmos. Environ.*, **14**, 397–400.

Monin, A. S., and A. M. Yaglom, 1971: *Statistical Fluid Mechanics: Mechanics of Turbulence*, Vol. I. MIT Press, 769 pp.

Orgill, M. M., 1981: Atmospheric studies in complex terrain: A planning guide for future studies. Rep. PNL-3656, Pacific Northwest Laboratories, Richland, WA, U.S. Department of Energy Contract DE-AC06-76RLO 1830.

Raynor, G. S., P. Michael and S. SethuRaman, 1980: Meteorological measurement methods and diffusion models for use at coastal nuclear reactor sites. *Nuclear Safety*, **21**, 749–765.

Schacher, G. E., K. L. Davidson and C. W. Fairall, 1980: Atmospheric marine boundary layer mixing rates in the California coastal region. Naval Postgraduate School Rep. No. NPS61-80-003, 115 pp.

——, C. W. Fairall, K. L. Davidson and T. M. Houlihan, 1978: Experimental investigation of the marine boundary layer in support of air pollution studies in the Los Angeles air basin. Naval Postgraduate School Rep. No. NPS61-78-002, 257 pp.

Schatzmann, M., 1979: An integral model of plume rise. *Atmos. Environ.*, **13**, 721–731.

Shair, F. H., E. Sasaki, D. Carlan, G. R. Cass, W. R. Goodin, J. Edinger and G. E. Schacher, 1981: Transport and dispersion of airborne pollutants associated with the land breeze-sea breeze system. *Atmos. Environ.* (in press).

Simmonds, P. G., G. R. Shoemake, J. E. Lovelock and H. C. Lord, 1972: Improvements in the determination of sulfur hexafluoride for use as a meteorological tracer. *Anal. Chem.*, **44**, 860–863.

Smith, T. B., S. L. Marsh, W. H. White, T. N. Jerskey, R. G. Lamb, P. A. Durbin and J. P. Killus, 1976: Analysis of the data from the three-dimensional gradient study. Final Report to the California Air Resources Board under Contracts ARB-4-051 and ARB-4-250, Meteorology Research, Inc., Pasadena, and Systems Applications, Inc., San Rafael, 124 pp.

Stull, R. B., 1973: Inversion rise model based on penetration convection. *J. Atmos. Sci.*, **30**, 1092–1099.

Venkatram, A., 1976: Internal boundary layer development and fumigation. *Atmos. Environ.*, **11**, 479–482.

Willis, G. E., and J. W. Deardorff, 1976a: Visual observations of horizontal planforms of penetration convection. *Preprints Third Symp. Atmospheric Turbulence Diffusion and Air Quality*, Raleigh, Amer. Meteor. Soc., 1–8.

——, and ——, 1976b: A laboratory model of diffusion into the convective planetary boundary layer. *Quart. J. Roy. Meteor. Soc.*, **102**, 427–445.

Zeman, O., and H. Tennekes, 1977: Parameterization of the turbulent energy budget at the top of the daytime atmospheric boundary layer. *J. Atmos. Sci.*, **34**, 111–123.